Marine Geology 394 (2017) 69–81

Contents lists available at ScienceDirect

Marine Geology

journal homepage: www.elsevier.com/locate/margo

Neogene fungal record from IODP Site U1433, South China Sea: Implications for paleoenvironmental change and the onset of the Mekong River

Y.F. Miao[a,b], S. Warny[a,c,*], C. Liu[a], P.D. Clift[a], M. Gregory[a,c]

[a] Department of Geology and Geophysics, Louisiana State University, E-235 Howe-Russell, Baton Rouge, LA 70803, USA
[b] Key Laboratory of Desert and Desertification, Cold and Arid Regions Environmental and Engineering Institute, Chinese Academy of Sciences, Lanzhou 730000, China
[c] Museum of Natural Science, Louisiana State University, 109 Foster Hall, Baton Rouge, LA 70803, USA

ARTICLE INFO

Keywords:
Fungal spores
Flux
Paleoenvironment
South China Sea
Neogene

ABSTRACT

The development of the Mekong River, although poorly constrained, plays a key role in our understanding of South China Sea drainage evolution. Here we attempt to improve our understanding of this evolution using a fungal spore record in the southwestern South China Sea at International Ocean Discovery Program (IODP) Site U1433. We present the variety of fungal morphologies extracted from the sediments and investigate their possible relationships with paleoenvironmental changes based on types, concentration and flux changes. Overall, > 30 morphologic types were found and are grouped into three basic assemblages: single-, double- and multi-celled spores. The spore fluxes continuously increase up-section, along with their diversity, although there are strong shorter fluctuations. One notable step in evolution is recorded at ca. 8 Ma. We argue that the trends in fungal flux are mainly linked to the strengthened terrestrial biomass input driven by tectonics rather than paleoclimate change and that this event is mainly linked to onset of the Mekong River in its present location.

1. Introduction

Fungal spores are often disregarded in the palynological literature where most of the focus in often placed on pollen, spores and single-celled organic-walled algae. Yet, fungal spores are widely distributed in the atmosphere, on the land surface, in water, caves or in soils. Animals and plants also serve as carriers of fungal spores, either on their surface or within their tissues. Furthermore, they have one of the longest geological records, as shown by a nearly two billion year old simple fungi assemblage found in Precambrian chert from the Gunflint Iron Formation of Lake Superior, USA (Oró et al., 1965). Despite the under-utilization of this microfossil, fungal spores are well known from several studies that have been carried out on a variety of materials at different time scales (e.g., Ainsworth et al., 1971; Cook et al., 2011; Cross et al., 1966; Edgcomb et al., 2011; Eshet et al., 1995; Gelorini et al., 2011; Graham, 1962; Jansonius and Kalgutkar, 2000; Lai et al., 2007; Mudie et al., 2002; Oró et al., 1965; Raghukumar et al., 2004; Taylor et al., 2014; Wolf, 1966). However, our knowledge of fungal spores is extremely limited with regard to their huge abundance (about 10 times larger than the species of angiosperm) and diversity in the terrestrial or marine realms. In this study of fungal spores from International Ocean Discovery Program (IODP) Site U1433, we examined the evolution of the terrestrial regions around the South China Sea in order to understand the tectonics of this basin, the climatic development of the area and the evolution of continental drainage systems.

The South China Sea, as one of largest marginal basins in SE Asia, receives much of the sediment that is being eroded from the Asian continent via a number of small and well-known larger river systems including the Pearl, Red, and Mekong Rivers (Métivier et al., 1999) (Fig. 1). The sedimentary record of this region can provide essential information on the evolution of tectonics, erosion, chemical weathering and climate of the adjacent continent (Clift, 2006; Wan et al., 2012; Wei et al., 2006). The South China Sea is also regarded as one of the primary sources of water vapor for the East Asian summer monsoon. Sediments from this basin thus provide critical information for investigating the opening of the South China Sea and the potentially linked development of the East Asian monsoon (Clift et al., 2008b; Luo and Sun, 2007; Wan et al., 2006, 2007).

In this study, we focus on fungal spores recovered from IODP Site U1433 in the central SW portion of the deep-water South China Sea basin (Fig. 1). These newly acquired Miocene records provide a unique chance to analyze fungal assemblages since ~17 Ma, and to supply information on fungal spore morphologies deposited in Neogene marine sediments. Variations in fungal assemblage are evaluated for their potential significance and geological implications within the depositional history in this deep-water basin.

* Corresponding author at: Department of Geology and Geophysics, Louisiana State University, E-235 Howe-Russell, Baton Rouge, Louisiana 70803, USA.
E-mail address: swarny@lsu.edu (S. Warny).

http://dx.doi.org/10.1016/j.margeo.2017.08.019

Available online 31 August 2017

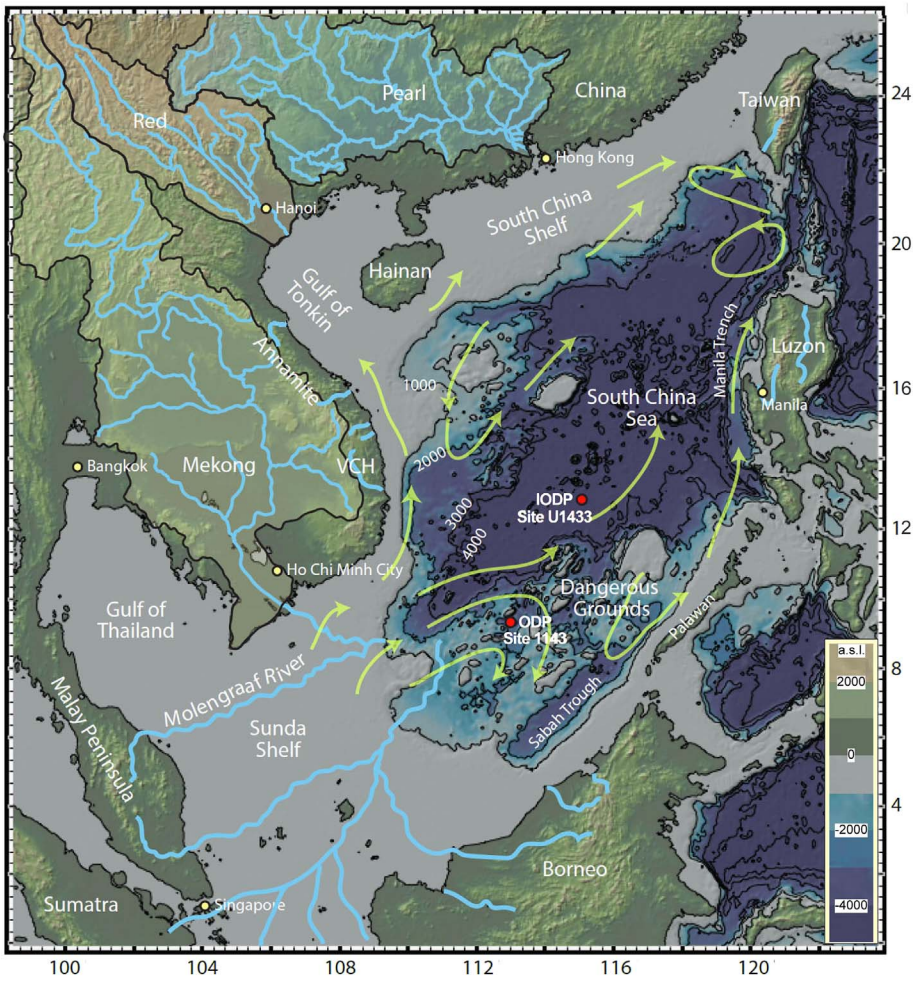

Fig. 1. Bathymetric map of the South China Sea showing the location of IODP Site U1433 and ODP Site 1143. Topography is from Shuttle Radar Topography Mission (SRTM) plotted by GeoMapApp. Major fluvial systems which deliver sediments into the South China Sea are also shown, together with the Molengraaff River of glacial age crossing the Sunda Shelf (Molengraaff and Weber, 1919). Green arrows show surface currents active during modern summer monsoon. Isobaths are shown in 1000 m intervals. Vietnamese Central Highlands = VCH.

2. Geological setting and materials

The region that today includes the South China Sea began to extend initially in the latest Cretaceous (Cullen et al., 2010), but underwent the main phase of continental rifting in the Eocene (Ru and Pigott, 1986; Su et al., 1989), culminating in the onset of seafloor spreading around 30 Ma along much of the southern Chinese margin (Briais et al., 1993; Li et al., 2014). Study of paleomagnetic data triggered a debate about when active seafloor spreading ended (Barckhausen et al., 2014), but drilling during IODP Expedition 349 now demonstrates that the opening was essentially completed at about 15 to 16 Ma (Li et al., 2014). Site U1433 overlies an oceanic basaltic basement dated at ~17 Ma based on microfossils in the overlying sediment (Li et al., 2015), and is located near the fossil seafloor spreading ridge. Seafloor spreading in the basin stopped shortly after the eruption of the basalt cored at our targeted drill site.

The causes of extension have been widely debated and have involved relative shear between Indochina and mainland Asia, as a result of the left lateral extrusion of the Indochina Block along the Red River Fault Zone (Replumaz and Tapponnier, 2003; Tapponnier et al., 1982). Alternatively, others have invoked subduction-related forces towards the south, causing the Dangerous Grounds continental block to rift from mainland Asia and subsequently collide with Borneo closing an earlier paleo-South China Sea basin at ~16 Ma (Clift et al., 2008a; Hutchison, 2004; Morley, 2002; Taylor and Hayes, 1983). Since the middle Miocene, the tectonics of the basin have been relatively inactive, with the exception of active subduction along the eastern edge of the basin where South China Sea lithosphere is still subducting beneath the Philippine arc (Hayes and Lewis, 1984). There have also been intraplate tectonic activities, most notably the uplift of the Vietnamese Central Highlands and the extrusion of a thick basaltic sequence mostly after ~8 Ma (Carter et al., 2000; Cung et al., 1998), although with lesser volumes of lava being emplaced in the early and middle Miocene (Hoang and Flower, 1998; Wang et al., 2001). Further intraplate magmatism in the form of seamounts is known until Quaternary times from the far SW (Li et al., 2013) to the NE of the basin (Yeh et al., 2012), as well as magmatism on Hainan Island (Tu et al., 1991). Compression along the southern side of the basin, along the northern coast and continental margin of Borneo, appears to be only slightly active in the present day (Hinz et al., 1989; Simons et al., 2007).

The relatively central location of Site U1433 within the oceanic basin means that several possible sources may have provided sediment to this location in the geologic past. Our working hypothesis was that the largest river in Southeast Asia, namely the Mekong, might be the primary source of sediment to the site, at least in the recent geological past (i.e., the last 17 Ma), because it is located only ~450 km to the southeast (Wan et al., 2006) and because the site is more distant from other large fluvial sources. This hypothesis is largely supported by the fact that sedimentary discharge from the Mekong is substantial (Milliman and Syvitski, 1992) and also by the fact that other potential sources, such as from Luzon or Borneo, are isolated from the site by significant bathymetric features such as the Manila Trench and the Sabah Trough (Fig. 1).

The development of river systems in East Asia is a controversial topic because rivers are sensitive to the development of topography and therefore to the uplift of the Tibetan Plateau, as well as the rifting of the marginal seas in Southeast Asia, leading to a regional scale tilting of the continent since the start of India-Asia collision. A number of different

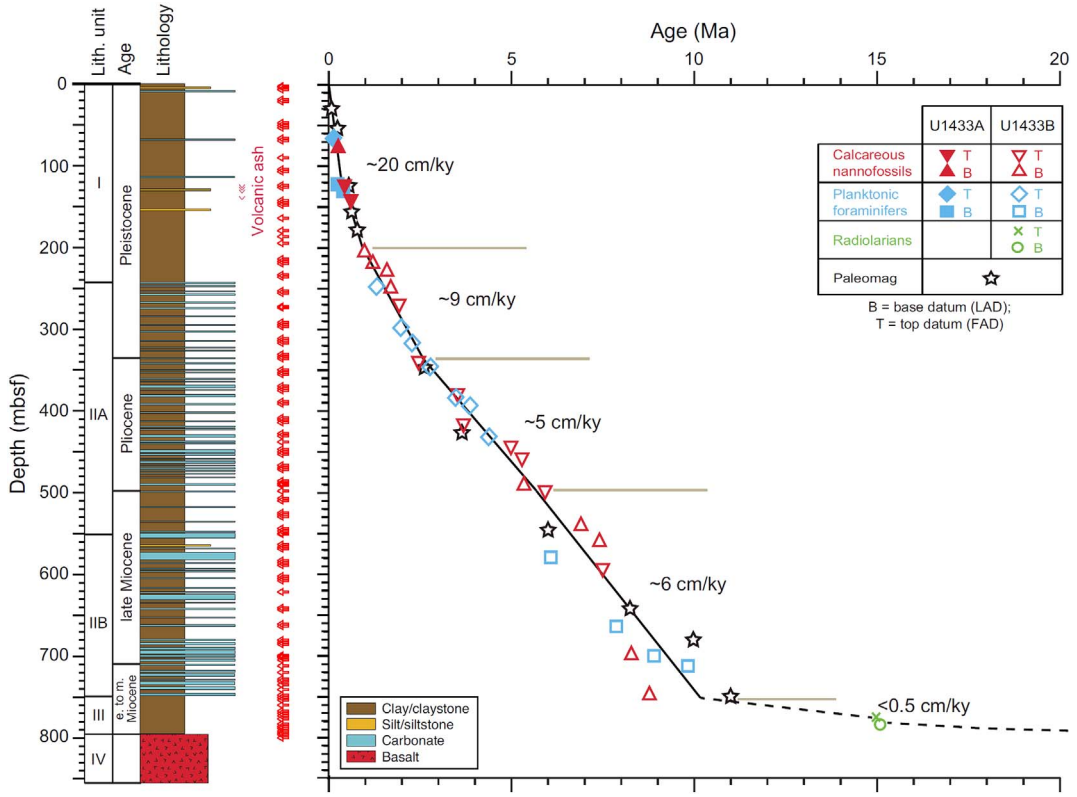

Fig. 2. Lithological column against age-depth model (after Li et al., 2015) and locations of fungal samples (red arrows) at Site U1433. FAD = first appearance datum, LAD = last appearance datum. (For interpretation of the references to color in this figure legend, the reader is referred to the web version of this article.)

lines of evidence now suggest that many of the major rivers that have their origins on the Tibetan Plateau have experienced headwater capture and in particular loss of headwater drainage from the Red River and transfer of this catchment into the neighboring systems (Clark et al., 2004; Brookfield, 1998; Zheng et al., 2013). Most of this capture occurred in the early Miocene, before around 24 Ma, although modern sediment transport routes between the Sunda shelf and the drill site would presently favor sediment transport from the Mekong River. The role of the Mekong River in this process, if any, is obscure because of the lack of long geological records from its delta/fan. Seismic-based investigations suggest that this is a relatively young system that has only been in place since the start of the Pliocene (Murray and Dorobek, 2004; Li et al., 2013), but there is little additional evidence. The development of the Mekong is poorly defined but plays a crucial part in our understanding of regional drainage evolution. We try to constrain this evolution using the fungal spore record at IODP Site U1433. This site is a good candidate for such a study because it recovered 800 m of uppermost lower Miocene to recent sediments overlying the oceanic basaltic basement (Li et al., 2015) (Fig. 2). The recovered sediment was divided into lithologic units based on macro- and microscopic observations of the cores combined with magnetostratigraphic data. Lithologic Unit I (0 to ~245 mbsf) consists of.dark greenish gray clay with interbedded very thin clayey silt. Unit II contains dark greenish gray clay and claystone with frequent medium to thick greenish gray nannofossil ooze and chalk interbeds. This unit is divided into upper and lower subunits based on the occurrence of thick to very thick (> 1 m) greenish gray nannofossil chalk interbeds in Subunit IIB, compared to thinner beds in Subunit IIA. Unit III consists of dominantly massive reddish and yellowish brown claystone and claystone with silt, with little coarser material present, occasional thin silty turbidites, and common dark staining associated with bioturbation. This unit lies directly on the basaltic basement (Unit IV) (Li et al., 2015).

Li et al. (2015), based on the on-board age model, indicates that extremely low sedimentation rates (< 0.5 cm/ky) characterize the early to middle Miocene. The sedimentation rates then fluctuate between ~5–6 and ~9 cm/ky in the late Miocene (starting at about 9.5 Ma) to early Pleistocene, and reach ~20 cm/ky during the middle and late Pleistocene (after ~2 Ma) (Fig. 2).

3. Palynological methods

A total of 116 bulk sediment samples (Fig. 2 and Table 1) were selected in order to provide an even distribution through the entire time interval recovered at IODP Site U1433. Samples were chemically processed following a palynological technique summarized by Brown (2008). For each sample, the available amount (ranging from 2.4 to 27.3 g) of dried sediment was weighed. The sediment was spiked with a known quantity of *Lycopodium* spores to allow assessment of the absolute abundance and the flux of organic-walled microfossils to the sample. Acid-soluble minerals were digested in hydrochloric acid (HCl) and hydrofluoric acid (HF) to remove carbonates and silicates respectively. The organic-walled microfossils were then concentrated by filtration through a 10-μm mesh sieve.

Fungal concentrations were calculated using the equation of Benninghoff (1962), $C = (Pc \times Lt \times T)/(Lc \times W)$, where C = concentration (specimens per gram of dried weight of sediment sampled, or gdw^{-1}), Pc = the number of fungal spores counted, Lt = the number of *Lycopodium* spores per tablet, T = the total number of *Lycopodium* tablets added per sample, Lc = the number of *Lycopodium* spores counted, W = the weight of dried sediment (with dried weight (dw) in grams).

In addition, fungal flux was calculated in order to describe the change of fungal assemblage through time. The fungal flux was calculated using the equation: $I = (Pc \times Lt \times T \times R \times S)/(Lc \times W)$, where I = flux (specimens/cm^2/ky, ky = 1000 years), Pc = the number of fungal spores counted, Lt = the number of *Lycopodium* spores per tablet, T = the total number of *Lycopodium* tablets added per sample, R = sedimentation rates; Lc = the number of *Lycopodium* spores

Table 1
Detailed information of number of fungal morphologies, concentrations and fluxes of fungi, IODP Site U1433.

Sample	Depth (m)	Age (Ma)		Concentrations				Influx			
			NM	SC	DC	MC	Total	SC	DC	MC	Total
1433A											
1H1W	2.783	0.001	4	4284	148	886	5318	42,843	1477	8864	53,185
1H3W	3.94	0.010	1	731	0	0	731	7075	0	0	7075
1H5W	6.97	0.018	2	488	0	98	585	5647	0	1129	6777
3H1W	19.09	0.043	8	4810	115	401	5325	75,134	1789	6261	83,184
3H3W	21.68	0.047	4	3001	0	931	3932	29,348	0	9108	38,456
6H1W	47.67	0.089	5	3756	0	791	4546	70,984	0	14,944	85,928
6H3W	50.68	0.094	5	4957	0	1538	6495	108,747	0	33,749	142,497
6H5W	53.72	0.099	6	2384	104	415	2902	47,823	2079	8317	58,219
8H1W	66.62	0.121	2	2348	0	511	2859	54,109	0	11,763	65,872
8H3W	69.62	0.160	1	619	0	0	619	11,398	0	0	11,398
10H5W	90.44	0.285	1	163	0	0	163	4713	0	0	4713
12H1W	104.53	0.376	5	1546	50	997	2593	35,121	1133	22,658	58,912
12H3W	107.42	0.386	3	703	0	92	795	16,344	0	2151	18,494
14H1W	123.95	0.446	5	4443	256	256	4956	110,278	6362	6362	123,002
14H3W	126.59	0.472	0	0	0	0	0	0	0	0	0
16H1W	142.64	0.616	2	2115	0	53	2168	53,126	0	1328	54,454
16H3W	145.55	0.635	5	3168	0	460	3628	82,245	0	11,939	94,184
16H5W	148.24	0.652	2	1607	0	73	1680	41,524	0	1887	43,412
18H3W	164.35	0.755	0	0	0	0	0	0	0	0	0
20H1W	179.56	0.851	3	4035	168	1513	5716	107,497	4479	40,311	152,287
1433B											
2R1W	186.8	0.897	8	8403	545	1323	10,270	234,608	15,206	36,929	286,743
3R1W	195	0.949	2	2029	0	72	2102	51,670	0	1845	53,516
5R1W	214.27	1.145	6	4345	0	1262	5607	119,492	0	34,691	154,183
5R3W	217.27	1.190	3	796	0	122	918	22,113	0	3402	25,516
5R5W	219.94	1.234	4	5451	0	461	5911	63,677	0	5381	69,058
7R1W	233.56	1.643	1	220	0	0	220	2668	0	0	2668
7R3W	236.26	1.658	0	0	0	0	0	0	0	0	0
9R1W	253.32	1.729	1	104	0	0	104	1100	0	0	1100
9R3W	256.02	1.730	7	3089	57	515	3661	37,972	703	6329	45,004
11R10W	272.38	1.978	5	1235	0	183	1418	15,560	0	2305	17,865
11R21W	273.92	1.990	2	382	0	38	420	4196	0	420	4616
13R1W	291.78	2.129	4	1832	0	701	2533	22,113	0	8455	30,568
13R3W	294.59	2.152	4	2521	0	1086	3607	30,037	0	12,939	42,976
13R5W	297.02	2.165	3	1797	0	513	2310	22,947	0	6556	29,504
15R1W	311.59	2.279	5	3213	40	161	3414	37,330	467	1867	39,664
15R3W	314.33	2.302	2	880	0	176	1056	10,361	0	2072	12,433
15R5W	317.09	2.325	2	1481	0	57	1538	17,091	0	657	17,748
17R1W	330.83	2.429	4	3456	0	899	4355	45,851	0	11,921	57,773
17R3W	333.78	2.456	6	1376	53	423	1852	16,829	647	5178	22,654
17R5W	336.13	2.480	1	109	0	0	109	1386	0	0	1386
19R1W	349.9	2.805	1	64	0	0	64	469	0	0	469
19R3W	352.91	2.880	2	0	0	900	900	0	0	6288	6288
19R5W	355.3	2.951	2	731	0	209	940	5278	0	1508	6786
21R1W	369.69	3.339	2	347	0	20	367	2179	0	128	2307
21R3W	372.46	3.419	1	823	0	0	823	5006	0	0	5006
21R5W	375.26	3.492	6	1350	42	1054	2446	9724	304	7597	17,624
23R1W	388.78	3.589	6	816	0	1468	2284	5872	0	10,569	16,441
23R3W	391.5	3.603	6	859	72	859	1790	6405	534	6405	13,343
25R1W	408.62	3.662	3	550	0	110	660	3975	0	795	4770
25R3W	411.1	3.680	2	141	0	47	188	979	0	326	1305
25R5W	414.27	3.692	6	883	98	1325	2306	6421	713	9632	16,766
27R1W	427.68	4.296	4	236	79	1022	1337	1653	551	7162	9365
27R3W	430.64	4.580	3	1365	0	94	1459	8880	0	612	9493
28R1W	438.00	4.800	3	110	0	37	146	767	0	256	1023
29R1W	446.98	5.138	3	254	0	51	304	1846	0	369	2215
29R3W	450.11	5.190	4	164	16	49	229	1118	112	335	1565
29R5W	452.85	5.250	1	318	0	0	318	1853	0	0	1853
31R1W	466.46	5.304	4	866	102	255	1222	6386	751	1878	9015
31R3W	469.4	5.309	2	278	0	69	347	2041	0	510	2551
31R5W	471.62	5.314	1	150	0	0	150	1148	0	0	1148
33R1W	485.57	5.340	1	42	0	0	42	328	0	0	328
33R3W	488.36	5.344	4	334	39	79	452	2078	245	489	2812
33R4W	489.58	5.347	3	315	0	270	584	2271	0	1946	4217
33R5W	490.95	5.350	1	221	0	0	221	1640	0	0	1640
34R2W	498.00	5.760	4	1383	518	3283	5184	10,023	3759	23,805	37,587
35R3W	507.03	6.117	4	1568	68	205	1841	13,512	587	1762	15,862
35R5W	509.9	6.194	3	368	0	163	531	3435	0	1527	4962
37R1W	524.59	6.554	2	1331	0	333	1664	11,151	0	2788	13,939
37R3W	526.98	6.614	3	620	0	387	1007	5434	0	3396	8831

(continued on next page)

Table 1 *(continued)*

Sample	Depth (m)	Age (Ma)		Concentrations				Influx			
			NM	SC	DC	MC	Total	SC	DC	MC	Total
37R5W	529.54	6.677	4	765	51	867	1684	7233	482	8197	15,912
39R1W	543.85	7.017	1	77	0	0	77	711	0	0	711
39R3W	546.85	7.085	4	1140	0	489	1629	10,638	0	4559	15,197
39R5W	549.78	7.130	3	309	44	750	1103	2807	401	6816	10,024
39R6W	550.84	7.175	3	610	0	356	965	5640	0	3290	8930
41R1W	563.46	7.425	3	938	0	469	1407	8187	0	4094	12,281
41R3W	566.38	7.436	3	524	225	449	1199	4927	2112	4223	11,262
41R5W	568.79	7.447	3	107	0	427	534	975	0	3902	4877
43R1W	583.14	7.499	2	–	–	–	–	–	–	–	–
43R3W	585.83	7.515	4	234	26	104	365	2280	253	1013	3547
43R5W	588.86	7.523	1	127	0	0	127	1154	0	0	1154
45R1W	602.14	7.610	1	24	0	0	24	227	0	0	227
45R3W	605.07	7.635	1	0	0	16	16	0	0	143	143
45R5W	607.68	7.655	2	568	0	49	618	5059	0	440	5499
47R1W	621.55	7.748	0	0	0	0	0	0	0	0	0
49R1W	640.89	7.886	3	304	0	101	406	3006	0	1002	4008
49R3W	643.15	7.905	2	1204	80	0	1284	11,668	778	0	12,445
51R1W	660.77	8.023	1	78	0	0	78	737	0	0	737
51R3W	663.52	8.046	5	1917	0	5272	7189	17,058	0	46,910	63,969
53R1W	680.37	8.161	3	981	196	392	1570	9612	1922	3845	15,379
53R3W	683.16	8.186	2	766	0	328	1095	7057	0	3024	10,082
53R5W	685.57	8.206	0	0	0	0	0	0	0	0	0
55R1W	699.14	8.450	0	0	0	0	0	0	0	0	0
55R2W	700.00	8.500	3	245	147	588	980	2498	1499	5996	9993
55R3W	701.8	8.758	1	111	0	0	111	1008	0	0	1008
55R5W	704.67	9.066	0	0	0	0	0	0	0	0	0
56R1W	712.00	9.600	1	47	0	0	47	455	0	0	455
57R2W	720.00	10.500	1	8	0	0	8	3	0	0	3
58R1W	728.14	11.120	0	0	0	0	0	0	0	0	0
58R3W	730.82	11.500	5	1906	272	5446	7625	640	91	1828	2559
58R6W	735.12	11.729	1	0	0	120	120	0	0	44	44
59R4W	741.00	12.250	3	4203	4203	4203	12,610	1429	1429	1429	4287
60R1W	747.72	12.500	5	400	0	12,410	12,810	133	0	4130	4263
60R3W	750.71	12.830	0	0	0	0	0	0	0	0	0
60R5W	753.71	13.050	0	0	0	0	0	0	0	0	0
61R4W	760.00	13.660	5	50	38	38	126	15	11	11	38
62R1W	767.19	14.117	0	0	0	0	0	0	0	0	0
62R3W	770.1	14.346	0	0	0	0	0	0	0	0	0
62R5W	772.97	14.581	0	0	0	0	0	0	0	0	0
63R1W	776.84	14.796	1	0	0	34	34	0	0	10	10
63R4W	783.00	15.010	1	0	0	3	3	0	0	1	1
64R1W	786.28	15.257	1	0	0	23	23	0	0	7	7
64R3W	788.47	15.378	0	0	0	0	0	0	0	0	0
64R5W	791.72	15.803	0	0	0	0	0	0	0	0	0
64R6W	794.00	16.000	0	0	0	0	0	0	0	0	0
65R1W	796.07	17.029	0	0	0	0	0	0	0	0	0
65R1W*	796.07	17.029	0	0	0	0	0	0	0	0	0

NM: number of morphologies; SC: Single-celled; DC: Double-celled; MC: Multi-celled; *: replicate sample.

counted, W = weight of dried sediment, S = dry density of sample (data from Li et al., 2015).

4. Palynological results

> 30 major types of fungal spore morphologies were recovered from the 116 samples analyzed (Table 1). These 30 major types show a great diversity, with about 80 morphologies, as illustrated in Figs. 3–5. Although we do not attempt to describe all the fungi in this paper, some of the morphotypes recovered are well known and include taxa such as *Coniochaeta* cf. *ligniaria*, *Sordaria ascospores*, *Hyploxylonites wolfei*, *Coniochaeta*, *Apiospora*, *Clastesporium*, *Spegazzinia*, *Diporotheca*, *Tetraploa aristata*, and *Meliolinites*. The assemblages are dominated by single- and double-celled spores, with only rare multi-celled spores present. Overall, a total of 16 out of 30 samples collected from the stratigraphic levels older than 8 Ma yielded fungal spores, with the first appearance of multi-celled fungal spores at 15 Ma, and that of single and double-celled fungi spores at 14 Ma. But the presence of fungal spores is sporadic until 8 Ma. In samples younger than 8 Ma, fungal spores are consistently present and the morphological diversity is high (Fig. 6a). (Note that in both Figs. 6 and 7, the logarithmic value of 1 was given for samples where there were no fungal spores recovered.) The lack of fungi could be caused by depositional factors such as diagenesis or oxidation prior to deposition, but if this was the main influencing factor, then we would see all palynomorphs (pollen, spores, dinoflagellate cysts and fungi) destroyed at the same time, irrespectively of their shape, and this is not the case.

Below we provide a description of the fungal groups recovered, divided into three basic morphological assemblages; single-celled spores, double-celled spores and other multi-celled (multicellular) spore morphologies.

There are no obvious trends in the numbers of fungal morphologic types recovered from sediment older than the Pleistocene, but starting around 2.6 Ma, a higher variability in the diversity of fungal spores recovered is clearly noted (Fig. 6a).

Abundance varies throughout the record, with concentrations ranging from 0 (no yield of fungal spores) to about 15,000 spores per grams of dried sediment. Most of the barren samples are older than

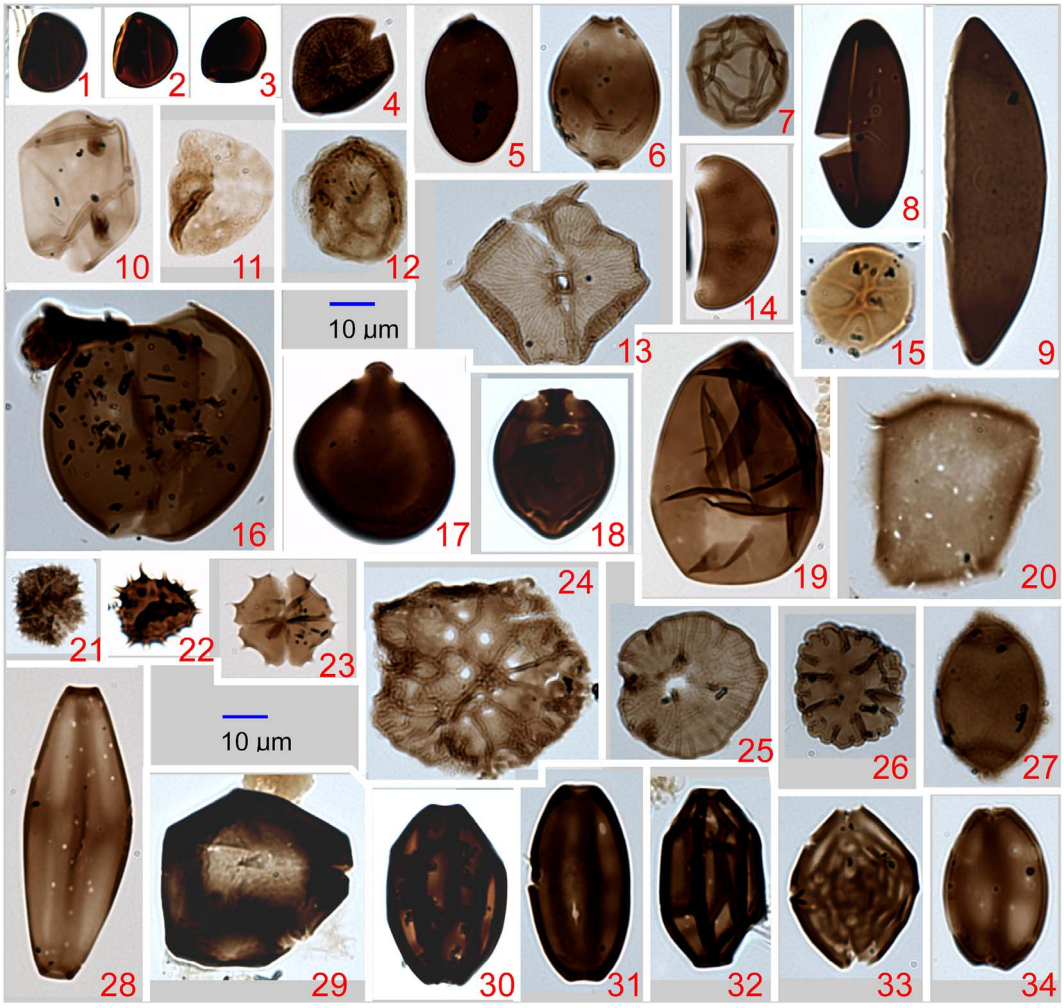

Fig. 3. Photomicrographs of single-celled fungal spores organized by morphological groups used in this study. Identification is provided when known. 1–3: *Exesisporites* (Jarzen and Elsik, 1986); 4, 5: *Polyporisporites* (Jarzen and Elsik, 1986) vs *Lacrimasporonites* (Sancay, 2014); 6: *Diporisporites* (Jarzen and Elsik, 1986); 7: unknown type; 8–9: *Hyploxylon*-type (Jarzen and Elsik, 1986); 10–11: *Psilodiporites krempii* (Kalgutkar, 1997); 12–13: unknown type; 14: *Hypoxylon*-type (Jarzen and Elsik, 1986); 15: unknown type; 16–18: *Biporisporites* (Wingate, 1983); 19: *Inapertisporites kedvesii* (Monga et al., 2015); 20: unknown type; 21–23: *Spegazzinia* type (Jarzen and Elsik, 1986); 24–27: unknown type; 28–34: *Striadiporites* (Jarzen and Elsik, 1986).

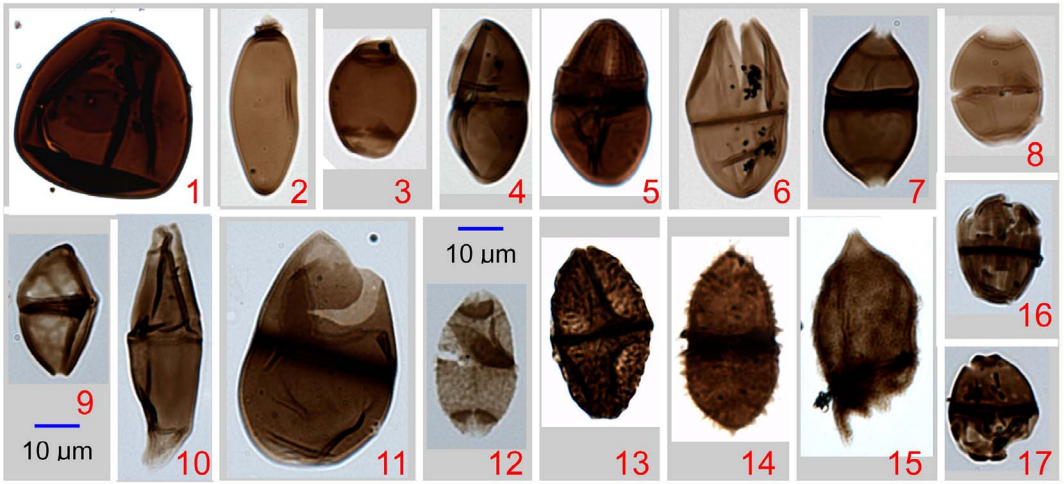

Fig. 4. Photomicrographs of double-celled fungal spores organized by morphological groups used in this study. Identification is provided when known. 1: *Diporisporites barrelis*? (Monga et al., 2015); 2: *Sordaria*; 3: unknown type; 4–6: *Delitschia*-type (Jarzen and Elsik, 1986); 7–11: *Dyadosporites* (Fernández, 1993; Jarzen and Elsik, 1986); 12–15: *Diornites* (Sancay, 2014).

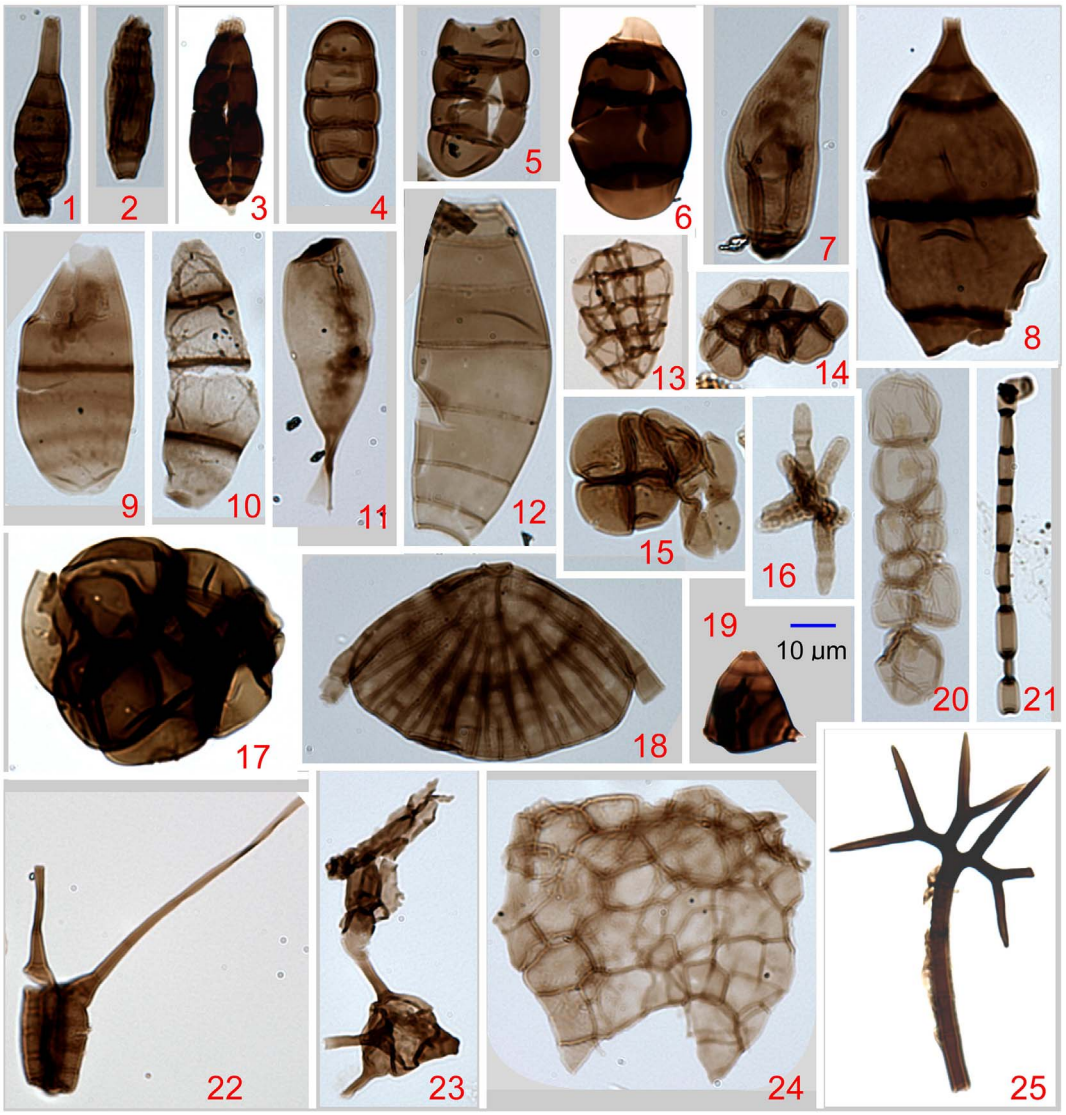

Fig. 5. Photomicrographs of multi-celled fungal spores organized by morphological groups used in this study. Identification is provided when known. 1: *Alternia* (Sancay, 2014); 2: *Diporicellaesporites jansonii* (Kalgutkar, 1997); 3: unknown type; 4: *Meliola* (Singh and Chauhan, 2008); 5: *Pluricellaesporites trichocladites* (Kalgutkar, 1997); 6–8: unknown type; 9–11: *Psilodiporites krempii* (Kalgutkar, 1997); 12: *Diporicellaesporite* (Kalgutkar, 1997); 13–19: unknown type; 22, 23: *Tetraploa aristata* (Ainsworth et al., 1971); 24: unknown type; 25: *Asterostromella investiens* (Ainsworth et al., 1971).

8 Ma, when clastic sedimentation rates were very slow. Out of 26 samples older than 8 Ma, 11 yielded single-celled types, five samples yielded double-celled types, and 10 samples contained multi-celled types. Concentrations in the time interval between ca. 17 and 8 Ma show strong fluctuations of 0–4200 grains/g, 0–1900 grains/g and 0–12,400 grains/g, for the three morphologic types respectively (Fig. 6a–c). In samples younger than 8 Ma, the concentrations of the three types continued to vary with strong fluctuations, especially in the younger sediments < 4 Ma, with a distribution up to 8400 grains/g (average of 1300 grains/g); up to 15,200 grains/g (average of 540 grains/g), and up to 3280 grains/g (average of 392 grains/g) respectively. The trends are similar when comparing total concentrations to that of single-celled morphologies (Fig. 6d).

The trend in fungal fluxes shows a strong pattern, with a major increase through time. Before 8 Ma, the maximum tabulated flux is 17,000 grains/cm^2/ky for single-celled spores, 1900 grains/cm^2/ky for the double-celled spores and 46,900 grains/cm^2/ky for the multi-celled spores (Fig. 7a-c). After 8 Ma, the maximum tabulated flux for the three respective types is of 234,600 grains/cm^2/ky (averaging 21,700 grains/cm^2/ky), 15,200 grains/cm^2/ky (averaging 540 grains/cm^2/ky) and 40,300 grains/cm^2/ky (averaging 5280 grains/cm^2/ky). The trends are similar when comparing the increase in flux to that of single-celled morphologies (Fig. 7d). The trends seen are thus mainly driven by the large increase in single-celled spore numbers. We further compared the total flux data of these three morphotypes (Fig. 8a) to the total organic carbon (Fig. 8b) and $^{87}Sr/^{87}Sr$ (Liu et al., 2017) (Fig. 8c) from the same hole, to the pollen fluxes from the Ocean Drilling Program (ODP) Site 1143 (Fig. 8d) located south of IODP Site U1433 (Fig. 1) (Luo and Sun, 2007), to sea-surface temperature change in the west Pacific Ocean (Zhang et al., 2014) (Fig. 8e) and to the global oxygen isotopic variability of the ocean (Zachos et al., 2008) (Fig. 8f). There are no obvious synchronous relationships between the record of total fungal fluxes and the total organic carbon (wt%), ratio of $^{87}Sr/^{87}Sr$ from the same hole as well as pollen fluxes from the ODP Site 1143, but the sea surface temperature and global ice volume/temperature trends do correlate with the total fungal flux.

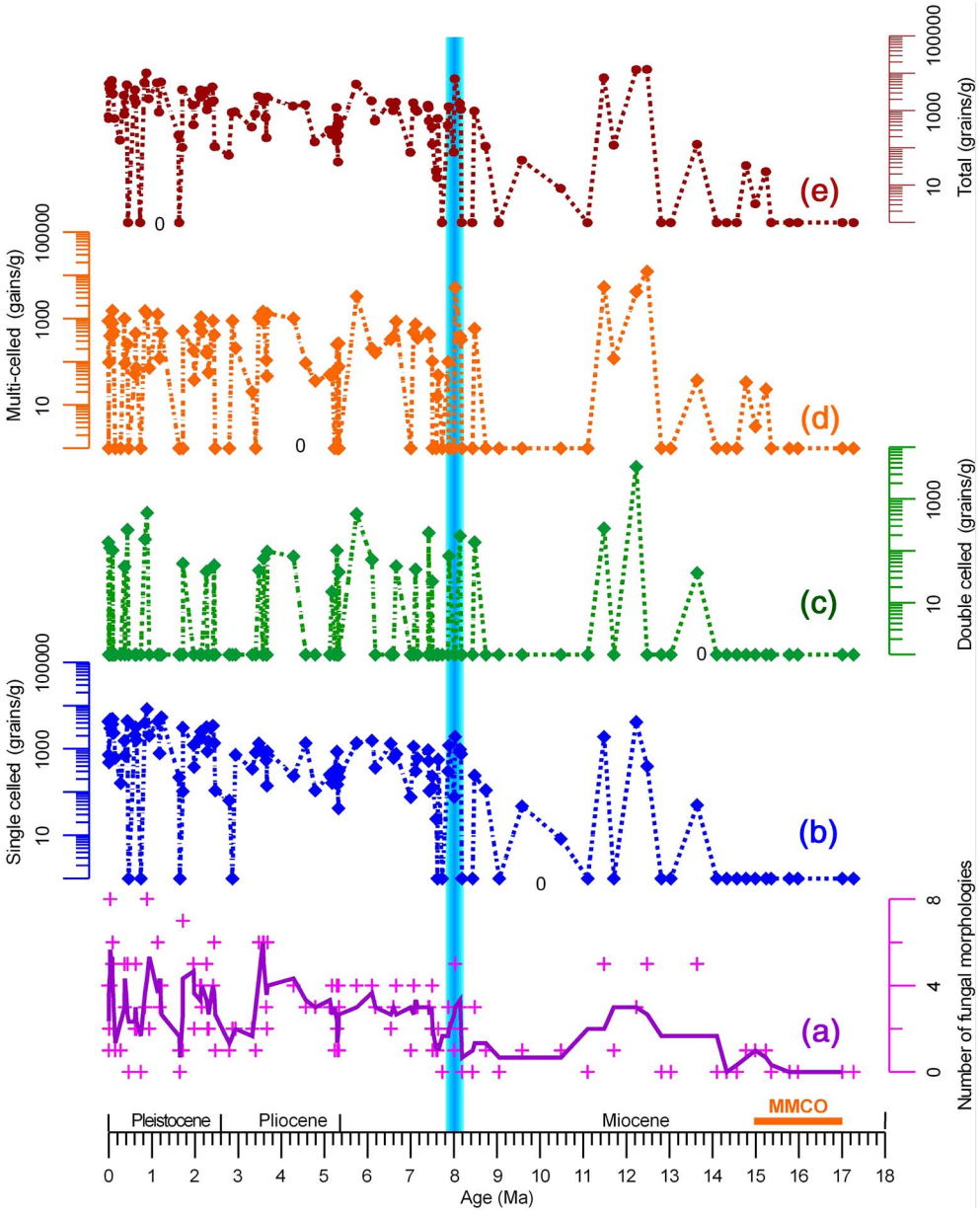

Fig. 6. Diagrams showing (a) the number of fungal morphologies observed in each sample (purple line is a 3-point running average), and concentrations of (b) single-celled, (c) double-celled, (d) multi-celled and (e) total fungal spores at Site U1433. MMCO: Middle Miocene Climatic Optimum. The shaded blue bar highlights the 8 Ma transition. (For interpretation of the references to color in this figure legend, the reader is referred to the web version of this article.)

5. Discussion

5.1. Fungal origins

Fungi are among the most widespread living eukaryotic organisms and can be found on the Earth's surface or within various media, including the air, soil, sand dunes, aquatic or marine realms, and even within animals and vegetation where they colonize numerous substrates and perform multiple functions (Cantrell et al., 2011). For example, they occur in habitats ranging from the Antarctic (Kochkina et al., 2012; Onofri et al., 2007) to salt flats to laminated organo-sedimentary ecosystems termed microbial mats. They have even been reported as epiphytes on unicellular or multi-celled plant hairs or trichomes (Pereira-Carvalho et al., 2009), in deep-sea ecosystems (Le Calvez et al., 2009; Nagano and Nagahama, 2012; Schumann et al., 2004) and buried 100 m deep in abyssal mud (Biddle et al., 2005). However, very little is known about the kinds of fungal spores that have been deposited in marine settings, or whether the fungal spores were transported to the sample location by rivers, oceanic currents, animals, atmospheric circulation, or if they originate from oceanic sources (e.g. fish fungi). This makes determining the source of fungal spores found at Site U1433 quite difficult.

Despite these issues, several factors allow us to confidently postulate that the majority of the fungal spores recovered from the studied marine sediments were brought there with the clastic sedimentary load delivered by rivers and transported by oceanic currents to deeper basins. First, the studied core was recovered in > 2000 m of water, and both the water and the constant influx of the sediment likely made it difficult to support living fungi to grow or penetrate through the sediments. Second, in addition to the fungal study, we also analyzed the sporopollen and dinoflagellate cysts from IODP Site U1433 and measured their concentrations and fluxes. The results show that variations in the fungal spore abundance are similar to those of the terrigenous sporopollenin, but different from the marine dinoflagellates (Miao et al., 2017, submitted, International Journal of Coal Geology). We thus postulate that most of the fungi originated from terrestrial sources and not the marine realm. Furthermore, geochemical and mineralogical records from Site U1433 also show that the sediment provenance changed greatly at 8 Ma and that the maximum erosion of material from the Mekong Basin occurred after 8 Ma (Liu et al., 2017), which

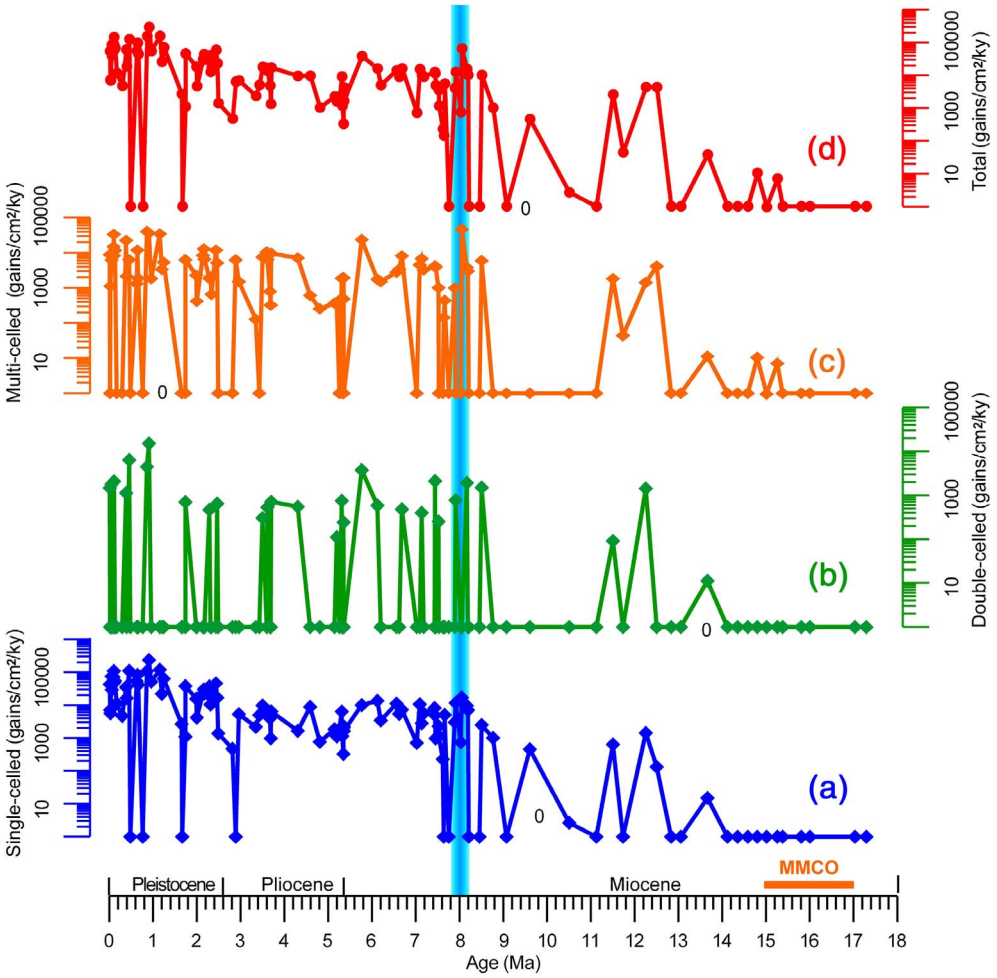

Fig. 7. Diagrams showing fluxes of (a) single-celled, (b) double-celled, (c) multi-celled and (d) total fungal spores at Site U1433. MMCO: Middle Miocene Climatic Optimum. The shaded blue bar highlights the 8 Ma transition.

correlates well with the fungal flux increase observed in our study. Finally, we compared the fungal spores recovered at Site U1433 with fungal spore morphologies described from the few detailed fungi studies available from this general area; i.e., a study of the Cenozoic of the Qaidam Basin, Central Asia (Zhu et al., 1985), as well as with unpublished fungal spore identifications from late Cenozoic palynological samples collected both from the Qaidam Basin and from the Yangtze River delta (Miao et al., 2016a; Zhang et al., 2013). Almost all single- and double-celled fungal spores are similar in both terrestrial sequences and from Site U1433. Only rare multi-celled fungal spores have been found in the terrestrial sediments. This is consistent with the idea that most single- and double-celled fungal spores do indeed originate from terrestrial sources. The source of the rare multi-celled fungal spores is uncertain, but overall, the similarity between our record and land records indicates that the bulk of the fungal spores at Site U1433 has a terrestrial provenance, as many of these species are commonly found growing on leaves (M. Blackwell, Herbarium of Louisiana State University, personal communication, 2016). As a result, the trends of fungal fluxes can be regarded as indicating a strengthened terrestrial biomass input.

5.2. Increasing fluxes and paleoclimate

Fig. 8 shows an overall covariance between the total fungal spore fluxes and sea-surface temperature (Zhang et al., 2014) as well as global $\delta^{18}O$ record (Zachos et al., 2008), potentially indicating that global climate significantly controls fungal abundances through time. If this was the case, two main climatic factors (temperature and moisture), could have affected the abundance of spores. Modern ecological shifts in fungi in relation to changes in temperature, precipitation and drought spells have been widely reported at spatiotemporal scales, including changes in length and timing of the growing season (Parmesan and Yohe, 2003; Walther, 2010). But unravelling the effects of climate variation on fungal distribution and fruiting is a major current challenge because of the complexity of fruiting phenology (Boddy et al., 2014), thus only large-scale trends are considered herein. For geological time scales (e.g., tectonics), temperature extremes (too hot or too cold) seem to be a major factor that can inhibit fungi from fruiting. It is thus possible that the low fluxes in fungal spores in the deeper part of the hole are a reflection of an interval known as the mid-Miocene Climatic Optimum (MMCO; ca. 17–15 Ma) (Flower and Kennett, 1994), where high temperature could have prevented fungi survival and/or reproduction. However, if this was strictly the case, fungal spores would not be found during other times of extreme warmth, such as during the Late Cretaceous, Paleocene-Eocene Thermal Maximum (PETM) or the Eocene because the temperatures during these periods are all much higher than during the MMCO (Mosbrugger et al., 2005; Zachos et al., 2008). However, there are in fact many reports of fungal fossils from those hyperthermal periods (e.g., Daghlian, 1978; Lange and Smith, 1975). Furthermore, the duration of low fungal fluxes at this site spans from ~17 to 8 Ma, much longer than the interval of the MMCO. Consequently, we discount temperature as the dominant control on fungal distribution at this site.

It is well known that moisture is important for fungal reproduction. Moisture inhibits activity when there is both too little and too much (Boddy et al., 2014). The question here is whether the East Asian summer monsoon played an important role in the abundance of fungal spores. Sporopollen assemblages can provide some insights. For

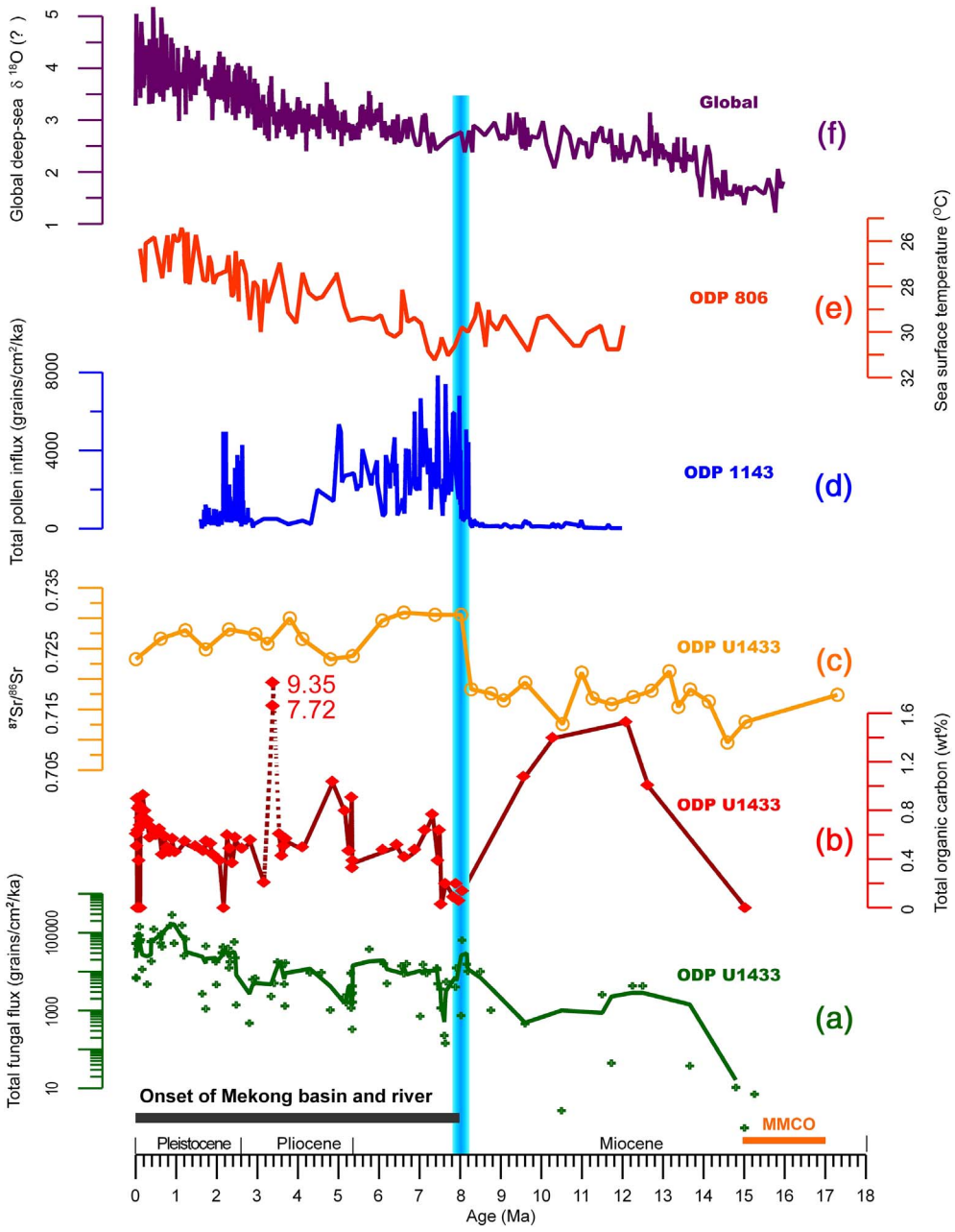

Fig. 8. Correlations among (a) the total fungal fluxes (dark green line: 3-point running meaning) (this study), (b) total organic carbon (wt%) by difference (CHNS-COUL) (Li et al., 2015), (c) $^{87}Sr/^{86}Sr$ measured on bulk sediments (Liu et al., 2017) from the Site U1433, (d) total pollen fluxes from ODP Site 1143 (Luo and Sun, 2007), (e) the sea surface temperature from ODP Site 806 in the west Pacific Ocean (Zhang et al., 2014) and (f) global ice volume/temperature change (Zachos et al., 2008, averaging every 11 values). The onset of Mekong River flux to the SW basin is from Liu et al. (2017). MMCO: Middle Miocene Climatic Optimum. The shaded blue bar highlights the 8 Ma transition.

example, the sporopollen assemblage is indicative of a conifer-dominated vegetation landscape in the arid Inner Asia (Miao et al., 2011, 2016a) and broadleaf-dominated forest in the semiarid Inner Asia (Hui et al., 2011) during the MMCO. The vegetation then dwindled as a result of global cooling (Miao et al., 2012). The percentages and spatial and temporal distribution of a unique palynomorph, the humid-tolerant *Fupingopollenites*, across Asia also support that the East Asian summer monsoon during the MMCO resulted in increased precipitation, followed by an important decrease during the mid-Miocene climatic transition (Miao et al., 2016b). If temperature and precipitation were the main control influencing fungal input, then fungal spores should increase during the MMCO; however, the fungal fluxes are lowest during this period.

In fact, for the event at ca. 8 Ma, some geochemical and mineralogical records from the South China Sea seem to show relatively complex patterns, e.g., at IODP Site U1433, the East Asian summer monsoon intensified after 8 Ma, reached a maximum at about 4 Ma, and then decreased afterwards (Liu et al., 2017). In contrast, other studies use chemical weathering constraints and erosion records to favor a strengthening as early as the early Miocene, ca. 23 Ma and a decrease in strength after 8–10 Ma (Clift et al., 2008b; Wan et al., 2007; Steinke et al., 2010). Pollen records from ODP Site 1143 are consistent with increased moisture and potentially with enhanced monsoonal activity since ca. 8 Ma (Luo and Sun, 2007), but whether this moisture is seasonal and monsoonal or more tropical is not clear. Monsoon records from the Himalaya and Loess Plateau (North China) indicate that the East Asian summer monsoon has changed in its distribution throughout the Neogene (An et al., 2001; Chen et al., 2007).

In summary, it is possible that the increased fungal flux signal at 8 Ma is coincident with a shift in regional climate after 8 Ma but additional records are needed to verify this hypothesis.

5.3. *Increasing fluxes and tectonics*

Tectonic events in the South China Sea may have contributed to the increased fungi flux trend seen in our record. Seafloor spreading in this

basin was thought to have ended at 20.5 Ma (Barckhausen et al., 2014) but the IODP drilling confirms younger estimates of a cessation around 17 to 15 Ma (Li et al., 2014, 2015). After the middle Miocene, tectonic activity in the basin became relatively weaker until the uplift of the Vietnamese Central Highlands and the extrusion of a thick basaltic sequence mostly after ~8 Ma (Carter et al., 2000; Cung et al., 1998). Such weakening in tectonic activity is reflected by decreasing volumes of lava emplacement (Hoang and Flower, 1998; Wang et al., 2001). At the same time tectonics drove long-term uplift and widening of the Tibetan Plateau, in the region where the headwaters of the Mekong River lie. Accelerated clastic sedimentary rates after 9.5 Ma indicate that Site U1433 received increasing amount of terrestrial sedimentary materials after that time, which is a trend opposite to that seen in the Pearl and Red River systems (Clift, 2006). Based on the $^{87}Sr/^{86}Sr$ (Fig. 8c) as well as other mineral and geochemical proxies, prior to 8 Ma the possible sources are complex (Liu et al., 2017), probably representing a mix from Indochina, the Dangerous Grounds and Palawan, but it seems clear that the Mekong Basin became the main contributor after 8 Ma, synchronous with the increasing trend in fungal fluxes. Therefore, we postulate that tectonics must have played a key role on the fungal distribution at Site U1433 through changes in the drainage system and associated sediment flux and fungal load.

5.4. Increasing fluxes and diagenesis

Sediments deposited in the marine realm can be rich in organic matter, as a result of the presence of various microfossils (e.g., fungi spores, algal cysts, spores and pollen), amorphous matter and resin (Thomas et al., 2015). Fig. 8b shows that the total organic carbon content decreases slightly in the upper ca. 1 Ma, which would be consistent with organic matter diagenesis (Li et al., 2015). Before ca. 2.1 Ma, total organic carbon is more variable, with a peak of over 7 wt % at ca. 3.37 Ma) (Li et al., 2015). Samples from these intervals are from carbonate turbidite deposits thought to have been derived from shallow-water locations south of Site U1433 (Li et al., 2015), i.e., within the Dangerous Grounds or Reed Bank.

If diagenesis and flux of carbonate turbidite deposits influenced the total organic carbon composition, then fungal spores could have been affected as well. It is indeed possible that the slow sedimentation prior to ~10 Ma would have provided the chance for spores to be oxidized and broken down prior to burial, potentially explaining their low abundance in the oldest sediments. Thus, we considered the fact that diagenesis could have affected our record in that portion of the cored interval, but the pollen, spores, and dinoflagellate cysts are well preserved throughout and there is no evidence that diagenesis played a significant role at these levels. Furthermore, we note that the low total fungal spore fluxes at depth contrasts with the high total organic carbon content found in the 12–10 Ma interval (Fig. 8b). However, we do recognize that the dramatic reduction in fungal abundance in sediments older than 8 Ma, rather than showing a more gradual reduction linked to age or burial depth, does call into question the importance of diagenesis.

5.5. Mekong River evolution

Overall, the most striking event based on the fungal spore record, and paralleled by clastic sedimentation, as well as geochemical and mineralogical provenance proxies (Liu et al., 2017), is the strong increase visible in fungal spores in sediments younger than ca. 8 Ma. In addition to higher fluxes, species concentrations and diversity are also higher after that time. We propose that the onset of Mekong River drainage into this portion of the South China Sea, driven by tectonic activity, is the leading factor behind this fungal spore record. Because the most likely change in climate is to a weaker summer monsoon after ~8 Ma, this is unlikely to have caused more fungal growth in any case.

Based on geochemical and mineralogical provenance data, Liu et al. (2017) argued that most of the sediments deposited at Site U1433 since 8 Ma were derived from the Mekong River, with lesser input from other small rivers draining coastal Vietnam, including the Central Highlands (Fig. 8c). Regional sediment budgets for this area (Luo and Sun, 2007; Clift, 2006; Ding et al., 2016) show a sharp increase in sedimentation rates at around this time, consistent with the Mekong either initiating or moving its mouth to the present location. Seismic evidence shows that major delta clinoforms have prograded across the modern shelf, starting close to the start of the Pliocene (~5 Ma; Murray and Dorobek, 2004; Li et al., 2013). Although this is somewhat later than the jump in flux described here we envisage that the river mouth initiated earlier further north and subsequently prograded to the shelf edge over time.

Another supporting line of evidence comes from the palynological record from ODP Site 1143. A dramatic increase in pollen fluxes is seen at that site at ca. 8 Ma (Fig. 8d). In their paper, Luo and Sun (2007) ascribed this event to tectonic deformation occurring around the southern South China Sea. They imply that tectonic activity onshore resulted in the rapid uplift of surrounding islands, mostly Borneo, as well as the Central Highlands of Vietnam, which would explain the higher fluxes of pollen. Certainly uplift of the Central Highlands would also have resulted in intensified fluvial run-off and a possible increase in sporopollen fluxes.

The increase in fungal spore fluxes at 8 Ma can be explained by higher Mekong River discharge into the South China Sea basin at that time, with the majority of the fungal spores originating from the landmass of central Indochina, rather than the headwaters on the Tibetan Plateau.

Why the Mekong River switched location at ~8 Ma is not clear. There is not much evidence for a significant uplift event in the headwaters, although the rising of the Central Highlands of Vietnam during the eruption of flood basalts around 8 Ma (Carter et al., 2000) may have played a role in displacing the river mouth to its present location.

6. Conclusion

Here we present a 17 million year fungal spore record deposited in the South China Sea and sampled at IODP Site U1433. About thirty types of fungal spores morphological groups were identified and divided into three basic morphological assemblages (single-celled, double-celled, and multi-celled spores). The distribution of the spores has been analyzed for possible relationships with paleoenvironmental changes in the region. Although the increase in fungal spore fluxes was likely affected by tectonics, the major increase seen at ca. 8 Ma likely primarily reflects the onset of the Mekong River in its present location, with lesser direct influence from an uplifting Central Highlands of Vietnam and diagenesis. The Mekong River is believed to have become the primary source of sediments to the southern South China Sea basin at that time. A weaker monsoon after 8 Ma is unlikely to have caused higher fungal production and fluxes.

Acknowledgments

This research used samples and/or data provided by the International Ocean Discovery Program (IODP). Funding for this research was provided by U.S. Science Support Program to Louisiana State University. The research was carried out at the Center for Excellence in Palynology (CENEX) in Baton Rouge, Louisiana. The visiting scholar fellowship to Yunfa Miao is funded by the Chinese Academy of Sciences through a partnership with CENEX. PC thanks the Charles T. McCord Jr. Chair in Petroleum Geology and USSAC for support during this study, plus D.K. Kulhanek and two anonymous reviewers.

References

Ainsworth, G.C., James, P.W., Hawksworth, D.L., 1971. Ainsworth & Bisby's, Dictionary

of the Fungi, Inlucidng the Lichens, 6th ed. Commonwealth Mycological Institute, Kew, Surrey, England.
An, Z., Kutzbach, J.E., Prell, W.L., Porter, S.C., 2001. Evolution of Asian monsoons and phased uplift of the Himalaya-Tibetan plateau since Late Miocene times. Nature 411, 62–66.
Barckhausen, U., Engels, M., Franke, D., Ladage, S., Pubellier, M., 2014. Evolution of the South China Sea: revised ages for breakup and seafloor spreading. Mar. Pet. Geol. 58, 599–611.
Benninghoff, W.S., 1962. Calculation of pollen and spores density in sediments by addition of exotic pollen in known quantities. Pollen Spores 6, 332–333.
Biddle, J., House, C., Brenchley, J., 2005. Microbial stratification in deeply buried marine sediment reflects changes in sulfate/methane profiles. Geobiology 3, 287–295.
Boddy, L., Büntgen, U., Egli, S., Gange, A.C., Heegaard, E., Kirk, P.M., ... Kauserud, H., 2014. Climate variation effects on fungal fruiting. Fungal Ecol. 10, 20–33.
Briais, A., Patriat, P., Tapponnier, P., 1993. Updated interpretation of magnetic anomalies and seafloor spreading stages in the South China Sea: implications for the tertiary tectonics of Southeast Asia. J. Geophys. Res. Solid Earth 98, 6299–6328.
Brookfield, M.E., 1998. The evolution of the great river systems of southern Asia during the Cenozoic India-Asia collision; rivers draining southwards. Geomorphology 22 (3–4), 285–312.
Brown, C.A., 2008. Palynological techniques. In: Riding, J.B., Warny, S. (Eds.), Am. Assoc. Strat. Palynologists, Second edition. .
Cantrell, S.A., Dianese, J.C., Fell, J., Gunde-Cimerman, N., Zalar, P., 2011. Unusual fungal niches. Mycologia 103, 1161–1174.
Carter, A., Roques, D., Bristow, C., 2000. Denudation history of onshore central Vietnam: constraints on the Cenozoic evolution of the western margin of the South China Sea. Tectonophysics 322, 265–277.
Chen, X., Fang, X., An, Z., Han, W., Wang, X., Bai, Y., Hong, Y., 2007. An 8.1 Ma calcite record of Asian summer monsoon evolution on the Chinese central Loess Plateau. Sci. China Ser. D Earth Sci. 50, 392–403.
Clark, M.K., Schoenbohm, L.M., Royden, L.H., Whipple, K.X., Burchfiel, B.C., Zhang, X., Tang, W., Wang, E., Chen, L., 2004. Surface uplift, tectonics, and erosion of eastern Tibet from large-scale drainage patterns. Tectonics 23, TC1006. http://dx.doi.org/10.1029/2002TC001402.
Clift, P.D., 2006. Controls on the erosion of Cenozoic Asia and the flux of clastic sediment to the ocean. Earth Planet. Sci. Lett. 241, 571–580.
Clift, P.D., Hodges, K.V., Heslop, D., Hannigan, R., Van Long, H., Calves, G., 2008a. Correlation of Himalayan exhumation rates and Asian monsoon intensity. Nat. Geosci. 1, 875–880.
Clift, P., Lee, G.H., Anh Duc, N., Barckhausen, U., Van Long, H., Zhen, S., 2008b. Seismic reflection evidence for a dangerous grounds miniplate: no extrusion origin for the South China Sea. Tectonics 27.
Cook, E.J., van Geel, B., van der Kaars, S., van Arkel, J., 2011. A review of the use of non-pollen palynomorphs in palaeoecology with examples from Australia. Palynology 35, 155–178.
Cross, A.T., Thompson, G.G., Zaitzeff, J.B., 1966. Source and distribution of palynomorphs in bottom sediments, southern part of Gulf of California. Mar. Geol. 4, 467–524.
Cullen, A., Reemst, P., Henstra, G., Gozzard, S., Ray, A., 2010. Rifting of the South China Sea: new perspectives. Pet. Geosci. 16, 273–282.
Cung, T., Dorobek, S., Richter, C., Flower, M., Kikawa, E., Nguyen, Y., McCabe, R., 1998. Paleomagnetism of Late Neogene basalts in Vietnam and Thailand: implications for the post-Miocene tectonic history of Indochina. In: Mantle Dynamics and Plate Interactions in East Asia, pp. 289–299.
Daghlian, C., 1978. A new melioloid fungus from the Early Eocene of Texas. Palaeontology 21, 171–176.
Ding, W., Li, J., Clift, P.D., Expedition, I., 2016. Spreading dynamics and sedimentary process of the Southwest Sub-basin, South China Sea: constraints from multi-channel seismic data and IODP Expedition 349. J. Asian Earth Sci. 115, 97–113.
Edgcomb, V.P., Beaudoin, D., Gast, R., Biddle, J.F., Teske, A., 2011. Marine subsurface eukaryotes: the fungal majority. Environ. Microbiol. 13, 172–183.
Eshet, Y., Rampino, M.R., Visscher, H., 1995. Fungal event and palynological record of ecological crisis and recovery across the Permian-Triassic boundary. Geology 23, 967–970.
Fernández, C.A., 1993. Fungal palynomorphs and algae from Holocene bottom sediments of Chascomús Lake, Buenos Aires province, Argentina. Palynology 17, 187–200.
Flower, B.P., Kennett, J.P., 1994. The middle Miocene climatic transition: East Antarctic ice sheet development, deep ocean circulation and global carbon cycling. Palaeogeogr. Palaeoclimatol. Palaeoecol. 108, 537–555.
Gelorini, V., Verbeken, A., van Geel, B., Cocquyt, C., Verschuren, D., 2011. Modern non-pollen palynomorphs from East African lake sediments. Rev. Palaeobot. Palynol. 164, 143–173.
Graham, A., 1962. The role of fungal spores in palynology. J. Paleontol. 60–68.
Hayes, D.E., Lewis, S.D., 1984. A geophysical study of the Manila Trench, Luzon, Philippines: 1. Crustal structure, gravity, and regional tectonic evolution. J. Geophys. Res. Solid Earth 89, 9171–9195.
Hinz, K., Fritsch, J., Kempter, E., Mohammad, M.A.M., Meyer, J., Mohamed, M.D., Vosberg, D.G.H., Weber, D.I.J., Benavidez, M.J., 1989. Thrust tectonics along the north-western continental margin of Sabah/Borneo. Geol. Rundsch. 78, 705–730.
Hoang, N., Flower, M., 1998. Petrogenesis of Cenozoic basalts from Vietnam: implication for origins of a 'diffuse igneous province'. J. Petrol. 39, 369–395.
Hui, Z.C., Li, J.J., Xu, Q.H., Song, C.H., Zhang, J., Wu, F.L., Zhao, Z.J., 2011. Miocene vegetation and climatic changes reconstructed from a sporopollen record of the Tianshui Basin, NE Tibetan Plateau. Palaeogeogr. Palaeoclimatol. Palaeoecol. 308, 373–382.
Hutchison, C.S., 2004. Marginal basin evolution: the southern South China Sea. Mar. Pet. Geol. 21, 1129–1148.
Jansonius, J., Kalgutkar, R., 2000. Redescription of some fossil fungal spores. Palynology 24, 37–47.
Jarzen, D.M., Elsik, W.C., 1986. Fungal palynomorphs recovered from recent river deposits, Luangwa Valley, Zambia. Palynology 10, 35–60.
Kalgutkar, R., 1997. Fossil fungi from the lower Tertiary Iceberg Bay Formation, Eukeka Sound Group, Axel Heiberg Island, Northwest Territories, Canada. Rev. Palaeobot. Palynol. 97, 197–226.
Kochkina, G., Ivanushkina, N., Ozerskaya, S., Chigineva, N., Vasilenko, O., Firsov, S., Spirina, E., Gilichinsky, D., 2012. Ancient fungi in Antarctic permafrost environments. FEMS Microbiol. Ecol. 82, 501–509.
Lai, X., Cao, L., Tan, H., Fang, S., Huang, Y., Zhou, S., 2007. Fungal communities from methane hydrate-bearing deep-sea marine sediments in South China Sea. ISME J. 1, 756–762.
Lange, R.T., Smith, P.H., 1975. Ctenosporites and other Paleogene fungal spores. Can. J. Bot. 53 (11), 1156–1157.
Le Calvez, T., Burgaud, G., Mahé, S., Barbier, G., Vandenkoornhuyse, P., 2009. Fungal diversity in deep-sea hydrothermal ecosystems. Appl. Environ. Microbiol. 75, 6415–6421.
Li, L., Clift, P.D., Nguyen, H.T., 2013. The sedimentary, magmatic and tectonic evolution of the Southwestern South China Sea revealed by seismic stratigraphic analysis. Mar. Geophys. Res. 34, 393–406.
Li, C., Xu, X., Lin, J., Sun, Z., Zhu, J., Yao, Y., Zhao, X., Liu, Q., Kulhanek, D.K., Wang, J., 2014. Ages and magnetic structures of the South China Sea constrained by deep tow magnetic surveys and IODP Expedition 349. Geochem. Geophys. Geosyst. 15, 4958–4983.
Li, C., Lin, J., Kulhanek, D., the Expedition 349 Scientists, 2015. Site U1433. In: Proceedings of the International Ocean Discovery Program. 349http://dx.doi.org/10.14379/iodp.proc.349.105.2015.
Liu, C., Clift, P.D., Murray, R.W., Blusztajn, J., Ireland, T., Wan, S.M., Ding, W.W., 2017. Geochemical evidence for initiation of the modern Mekong delta in the southwestern South China Sea after 8 Ma. Chem. Geol. 451, 38–54.
Luo, Y., Sun, X., 2007. Deep sea pollen record during 12–1.6 Ma from the southern South China Sea and its response to environmental change. Chin. Sci. Bull. 52, 2115–2122.
Métivier, F., Gaudemer, Y., Tapponnier, P., Klein, M., 1999. Mass accumulation rates in Asia during the Cenozoic. Geophys. J. Int. 137, 280–318.
Miao, Y.F., Fang, X.M., Herrmann, M., Wu, F.L., Zhang, Y., Liu, D.L., 2011. Miocene pollen record of KC-1 core in the Qaidam Basin, NE Tibetan Plateau and implications for evolution of the East Asian monsoon. Palaeogeogr. Palaeoclimatol. Palaeoecol. 299 (1), 30–38.
Miao, Y., Herrmann, M., Wu, F., Yan, X., Yang, S., 2012. What controlled Mid–Late Miocene long-term aridification in Central Asia?—global cooling or Tibetan Plateau uplift: a review. Earth Sci. Rev. 112 (3), 155–172.
Miao, Y., Fang, X., Liu, Y.-S.C., Yan, X., Li, S., Xia, W., 2016a. Late Cenozoic pollen concentration in the western Qaidam Basin, northern Tibetan Plateau, and its significance for paleoclimate and tectonics. Rev. Palaeobot. Palynol. 231, 14–22.
Miao, Y.F., Song, C.H., Fang, X.M., et al., 2016b. Late Cenozoic genus *Fupingopollenites* development and its implications for the Asian summer monsoon evolution. Gondwana Res. 29, 320–333.
Miao, Y.F., Warny, S., Gregory, M., Clift, P.D., Liu, C., 2017. Climatic or tectonic control on kerogen deposition in the South China Sea? A lesson learned from a comprehensive Neogene kerogen study of IODP Site U1433. Int. J. Coal Geol (under review).
Milliman, J.D., Syvitski, J.P., 1992. Geomorphic/tectonic control of sediment discharge to the ocean: the importance of small mountainous rivers. J. Geol. 525–544.
Molengraaff, G.A.F., Weber, M., 1919. Het verband tusschen den plistoceenen ijstijd en het ontstaan der Soenda-zee (Java-en Zuid-Chineesche Zee) en de invloed daarvan op de verspreiding der koraalriffen en op de land-en zoetwater-fauna. In: Verslag Van de Gewone Vergaderingen der Wis-En Natuurkundige Afdeeling. 28. pp. 497–544.
Monga, P., Kumar, M., Prasad, V., Joshi, Y., 2015. Palynostratigraphy, palynofacies and depositional environment of a lignite-bearing succession at Surkha Mine, Cambay Basin, north-western India. Acta Palaeobot. 55, 183–207.
Morley, C., 2002. A tectonic model for the Tertiary evolution of strike–slip faults and rift basins in SE Asia. Tectonophysics 347, 189–215.
Mosbrugger, V., Utescher, T., Dilcher, D.L., 2005. Cenozoic continental climatic evolution of Central Europe. Proc. Natl. Acad. Sci. 102 (42), 14964–14969.
Mudie, P.J., Rochon, A., Aksu, A.E., Gillespie, H., 2002. Dinoflagellate cysts, freshwater algae and fungal spores as salinity indicators in Late Quaternary cores from Marmara and Black seas. Mar. Geol. 190, 203–231.
Murray, M.R., Dorobek, S.L., 2004. Sediment supply, tectonic subsidence, and basin-filling patterns across the southwestern South China Sea during Pliocene to recent time. In: Clift, P., Wang, P., Kuhnt, W., Hayes, D. (Eds.), Continent-ocean interactions within east Asian marginal seas. Geophysical Monograph American Geophysical Union, Washington, DC, pp. 235–254.
Nagano, Y., Nagahama, T., 2012. Fungal diversity in deep-sea extreme environments. Fungal Ecol. 5, 463–471.
Onofri, S., Zucconi, L., Selbmann, L., de Hoog, S., de los Ríos, A., Ruisi, S., Grube, M., 2007. Fungal associations at the cold edge of life. In: Algae and Cyanobacteria in Extreme Environments. Springer, pp. 735–757.
Oró, J., Nooner, D., Zlatkis, A., Wikström, S., Barghoorn, E., 1965. Hydrocarbons of biological origin in sediments about two billion years old. Science 148, 77–79.
Parmesan, C., Yohe, G., 2003. A globally coherent finger-print of climate change impacts across natural systems. Nature 421, 37–42.
Pereira-Carvalho, R.C., Sepúlveda-Chavera, G., Armando, E.A., Inácio, C.A., Dianese, J.C., 2009. An overlooked source of fungal diversity: novel hyphomycete genera on trichomes of cerrado plants. Mycol. Res. 113, 261–274.
Raghukumar, C., Raghukumar, S., Sheelu, G., Gupta, S., Nath, B.N., Rao, B., 2004. Buried

in time: culturable fungi in a deep-sea sediment core from the Chagos Trench, Indian Ocean. Deep-Sea Res. I Oceanogr. Res. Pap. 51, 1759–1768.
Replumaz, A., Tapponnier, P., 2003. Reconstruction of the deformed collision zone between India and Asia by backward motion of lithospheric blocks. J. Geophys. Res. Solid Earth 108.
Ru, K., Pigott, J.D., 1986. Episodic rifting and subsidence in the South China Sea. AAPG Bull. 70, 1136–1155.
Sancay, R.H., 2014. The occurrence of Mediaverrunites in the Upper Miocene of the Black Sea, Turkey. Palynology 38, 28–37.
Schumann, G., Manz, W., Reitner, J., Lustrino, M., 2004. Ancient fungal life in North Pacific Eocene oceanic crust. Geomicrobiol J. 21, 241–246.
Simons, W., Socquet, A., Vigny, C., Ambrosius, B., Haji Abu, S., Promthong, C., Subarya, C., Sarsito, D., Matheussen, S., Morgan, P., 2007. A decade of GPS in Southeast Asia: resolving Sundaland motion and boundaries. J. Geophys. Res. Solid Earth 112.
Singh, S.K., Chauhan, M., 2008. Fungal remains from the Neogene sediments of Mahuadanr Valley, Latehar District, Jharkhand, India and their palaeoclimatic significance. J. Palaeontol. Soc. India 53, 73–81.
Steinke, S., Groeneveld, J., Johnstone, H., Rendle-Bühring, R., 2010. East Asian summer monsoon weakening after 7.5 Ma: evidence from combined planktonic foraminifera Mg/Ca and $\delta^{18}O$ (ODP Site 1146; northern South China Sea). Palaeogeogr. Palaeoclimatol. Palaeoecol. 289 (1–4), 33–43.
Su, D., White, N., McKenzie, D., 1989. Extension and subsidence of the Pearl River mouth basin, northern South China Sea. Basin Res. 2, 205–222.
Tapponnier, P., Peltzer, G., Le Dain, A., Armijo, R., Cobbold, P., 1982. Propagating extrusion tectonics in Asia: new insights from simple experiments with plasticine. Geology 10, 611–616.
Taylor, B., Hayes, D.E., 1983. Origin and history of the South China Sea basin. In: The Tectonic and Geologic Evolution of Southeast Asian Seas and Islands: Part 2, pp. 23–56.
Taylor, T.N., Krings, M., Taylor, E.L., 2014. Fossil fungi. Academic Press.
Thomas, M.L., Pocknall, D.T., Warny, S., Bentley Sr., S.J., Droxler, A.W., Nittrouer, C.A., 2015. Assessing palaeobathymetry and sedimentation rates using palynomaceral analysis: a study of modern sediments from the Gulf of Papua, offshore Papua New Guinea. Palynology 39, 410–433.
Tu, K., Flower, M.F.J., Carlson, R.W., Zhang, M., Xie, G., 1991. Sr, Nd, and Pb isotopic compositions of Hainan basalts (south China): implications for a subcontinental lithosphere Dupal source. Geology 19, 567–569.
Walther, G.R., 2010. Community and ecosystem responses to recent climate change. Philos. Trans. R. Soc. B 365, 2019–2024.
Wan, S., Li, A., Clift, P.D., Jiang, H., 2006. Development of the East Asian summer monsoon: evidence from the sediment record in the South China Sea since 8.5 Ma. Palaeogeogr. Palaeoclimatol. Palaeoecol. 241, 139–159.
Wan, S., Li, A., Clift, P.D., Stuut, J.-B.W., 2007. Development of the East Asian monsoon: mineralogical and sedimentologic records in the northern South China Sea since 20 Ma. Palaeogeogr. Palaeoclimatol. Palaeoecol. 254, 561–582.
Wan, S., Clift, P.D., Li, A., Yu, Z., Li, T., Hu, D., 2012. Tectonic and climatic controls on long-term silicate weathering in Asia since 5 Ma. Geophys. Res. Lett. 39.
Wang, J.H., Yin, A., Harrison, T.M., Grove, M., Zhang, Y.-Q., Xie, G.-H., 2001. A tectonic model for Cenozoic igneous activities in the eastern Indo–Asian collision zone. Earth Planet. Sci. Lett. 188, 123–133.
Wei, G., Li, X.H., Liu, Y., Shao, L., Liang, X., 2006. Geochemical record of chemical weathering and monsoon climate change since the early Miocene in the South China Sea. Paleoceanography 21.
Wingate, F.H., 1983. Palynology and age of the Elko Formation (Eocene) near Elko, Nevada. Palynology 7, 93–132.
Wolf, F.A., 1966. Fungus spores in East African lake sediments. Bull. Torrey Bot. Club 104–113.
Yeh, Y.C., Hsu, S.K., Doo, W.B., Sibuet, J.C., Liu, C.S., Lee, C.S., 2012. Crustal features of the northeastern South China Sea: insights from seismic and magnetic interpretations. Mar. Geophys. Res. 33 (4), 307–326.
Zachos, J.C., Dickens, G.R., Zeebe, R.E., 2008. An early Cenozoic perspective on greenhouse warming and carbon-cycle dynamics. Nature 451, 279–283.
Zhang, P., Miao, Y., Zhang, Z., Lu, S., Zhang, Y., Chen, H., Li, X., Miao, Q., Feng, W., Ou, J., Gong, X., Jiang, B., Li, W., 2013. Late Cenozoic sporopollen records in the Yangtze River Delta, East China and implications for East Asian summer monsoon evolution. Palaeogeogr. Palaeoclimatol. Palaeoecol. 388, 153–165.
Zhang, Y.G., Pagani, M., Liu, Z., 2014. A 12-million-year temperature history of the tropical Pacific Ocean. Science 344, 84–87.
Zheng, H., Clift, P.D., Tada, R., Jia, J.T., He, M.Y., Wang, P., 2013. A pre-Miocene birth to the Yangtze River. Proc. Natl. Acad. Sci. 1–6.
Zhu, Z., Wu, L., Xi, P., Song, Z., Zhang, Y., 1985. A Research on Tertiary Palynology from the Qaidam Basin, Qinghai Province. The Petroleum Industry Press, pp. 1–297.